Nonenhanced ECG-gated time-resolved 4D Steady-state free precession (SSFP) MR angiography (MRA) for assessment of cerebral collateral flow: comparison with digital subtraction angiography (DSA)

Rotem Shlomo Lanzman · Patric Kröpil · Peter Schmitt · Xiaoming Bi · Michael Gliem · Falk R. Miese · Daniel Hänggi · Marcel Kamp · Axel Scherer · Bernd Turowski · Dirk Blondin

Abstract

Objectives To evaluate a nonenhanced time-resolved 4D SSFP MRA for dynamic visualization of intracranial collateral blood flow.

Methods 22 patients (59.0±11.8 years) with steno-occlusive disease of brain-supplying arteries were included in this study. 4D SSFP MRA of the intracranial arteries was acquired with 15 temporal phases and a temporal resolution of 115 ms using 1.5 T MR. Cerebral DSA served as the reference standard and was available in all patients.

Results Nonenhanced 4D SSFP MRA allowed for detailed dynamic visualization of blood flow in the circle of Willis and its branches in 21 of 22 (95.5%) patients. Collateral flow was excluded with both 4D SSFP MRA and DSA in 4 patients. In 17 patients, DSA detected anterior collateral flow ($n=8$), posterior collateral flow via the right ($n=8$) and left ($n=7$) posterior communicating artery as well as patent EC-IC bypasses ($n=8$). 29 of 31 collateral flow pathways were visualized by 4D SSFP MRA. As compared to DSA, 4D SSFP MRA showed a high sensitivity (92.3%), specificity (100%), positive predictive value (100%) and negative predictive value (95.2%) for visualization of intracranial collateral flow.

Conclusions 4D SSFP MRA is a promising non-invasive imaging technique for dynamic visualization of intracranial collateral flow.

Keyword Nonenhanced MRA · Time-resolved MRA · Steady state free precession (SSFP) · Cerebral arteries · Digital subtraction angiography

R. S. Lanzman (✉) · P. Kröpil · F. R. Miese · A. Scherer · B. Turowski · D. Blondin
Department of Radiology, University Hospital Düsseldorf,
Moorenstr. 5,
40225 Düsseldorf, Germany
e-mail: rotemshlomo@yahoo.de

P. Schmitt
Siemens AG, Healthcare Section,
Erlangen, Germany

X. Bi
Siemens Healthcare,
Chicago, IL, USA

M. Gliem
Department of Neurology, University Hospital Düsseldorf,
Düsseldorf, Germany

D. Hänggi · M. Kamp
Department of Neurosurgery, University Hospital Düsseldorf,
Düsseldorf, Germany

Introduction

Stroke is one of the leading causes of mortality and disability in the western world [1]. Arteriosclerotic carotid artery disease is an important risk factor for stroke [2]. In case of hemodynamically significant stenosis or occlusion of brain-supplying arteries, the circle of Willis is the primary collateral pathway to maintain cerebral perfusion, while other collateral circulations include the external carotid artery and leptomeningeal anastomoses [3]. Conventional digital subtraction angiography (DSA) is considered as the gold standard for assessment of the carotid arteries and the intracranial circulation due to its high temporal and spatial resolution. However, as an invasive technique DSA exposes the patient to potential procedural

risks, as for example thromboembolic complications [4]. Therefore, non invasive imaging techniques as Doppler sonography, CT angiography (CTA) and MR angiography (MRA) are generally used as primary imaging modalities for assessment of the carotid and cerebral arteries. CTA and single phase Gd-enhanced enable visualization of the cervical and intracranial arteries with a large coverage, but do not provide direct haemodynamic information. With time-resolved contrast-enhanced MRA both anatomic and hemodynamic information can be obtained with extensive coverage [5–7]. However, the temporal resolution generally ranges between 0.5 and 2 sec, which might be not sufficient to depict intracranial collateral pathways. In addition, in patients with a glomerular filtration rate (GFR) of less than 30 ml/min the application of gadolinium-based contrast agent is considered problematic due to the potential risk for the development of nephrogenic systemic fibrosis (NSF) [8, 9]. Recently, steady-state free precession (SSFP) techniques have emerged as promising nonenhanced MR angiography methods and have shown promising results in various vascular territories, including the carotid, renal and coronary arteries [10–14].

Arterial spin labelling (ASL) techniques are usually applied to determine tissue perfusion using blood as an endogenous contrast material. With ASL, imaging contrast depends on the difference from measurements with and without magnetic labelling [15]. ASL techniques with varying delay times in combination with ECG-gated SSFP MRA techniques may provide dynamic MR angiographies, yielding both hemodynamic and anatomical information [16, 17]. The purpose of this study was to evaluate a non-contrast-enhanced time-resolved 4D steady-state free precession MRA (4D SSFP MRA) for dynamic visualization of intracranial collateral flow in patients with stenoocclusive disease of brain-supplying arteries in comparison to conventional DSA.

Material and methods

Two Siemens employees (P.S (Siemens AG, Healthcare Section, Erlangen, Germany) and X.B. (Siemens Healthcare, Chicago, IL, USA)) assisted in the development of this MR technique. Only the other authors had full control of the entire information and data submitted for publication.

This prospective study was approved by the institutional review board and written informed consent was obtained from all patients. The general contraindications for MR were applied and defined as exclusion criteria.

Between October 2009 and May 2010, 22 patients (5 women, 17 men, mean age 59.0±11.8 years) with stenoocclusive disease of brain-supplying arteries scheduled for cerebral DSA were included in this study. Indications for

DSA included control of EC-IC bypasses (n=6) and assessment of stenoocclusive disease of brain-supplying arteries (n=15). In addition, one patient that underwent DSA following surgical resection of an aneurysm of the left vertebral artery was also included in this study. In these 22 patients, 23 MR examinations were performed, as one patient was examined twice; in this patient, the first MR examination was performed three days after diagnostic DSA and the second MR examination two days after interventional stent placement in the right carotid artery. MR examinations were performed either before (n=5) or after (n=18) DSA, depending on the availability of patients and MR facilities. The time interval between DSA and MRA ranged between 0 and 113 days (mean time interval 11.6±24.5 days).

Conventional DSA

DSA was performed on a biplane angiography system (Integris Allura Biplane, Philips Healthcare) in all patients. Catheter-based selective visualization of the anterior and posterior circulation was performed by manual delivery of 8–10 ml iodinated contrast agent iohexol per run (Accupaque 300, GE Healthcare, Little Chalford, UK). In patients following EC-IC bypass surgery, selective angiograms of the external carotid artery were performed additionally for assessment of the EC-IC bypass.

MR angiography

All MR examinations were performed at 1.5 T (MAGNETOM Avanto, Siemens AG, Healthcare Sector, Erlangen, Germany). All subjects were studied in supine position with a 12-element head matrix coil. ECG electrodes were attached to the subjects' chest prior to the examination.

Following standard localizer images, a T2-weighted TSE sequence of the brain (TR/TE 5500/102 ms; slice thickness 5 mm) was acquired.

For 4D SSFP MR angiography, two magnetization-prepared and ECG-triggered 4D datasets were acquired with a TrueFISP CINE sequence in segmented fashion [17]. In each cardiac cycle, upon detection of the ECG R-wave, an inversion preparation pulse was played out followed by acquisition of N temporal phases. Within each temporal phase, a certain number of segments (=PE lines per phase) were acquired, so that a total of (N*segments) repetition intervals were carried out to sample the inversion recovery course after the magnetization preparation. With this procedure, two series of 3D datasets were sampled sequentially, one during recovery after non-selective inversion and another after slab-selective inversion (Fig. 1). This labeling scheme corresponds to the FAIR principle, which was originally published in the context of a brain perfusion study [18].
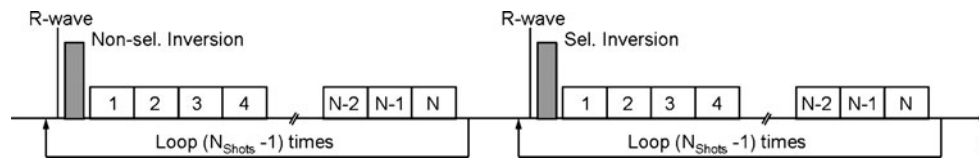
Fig. 1 Schematic display of the used sequence: First, a series of 3D datasets at multiple TI times is obtained for non-selective inversion. This is accomplished by repeating the magnetization and readout

(Nshots-1) times, until all data is acquired. This procedure is repeated for slice-selective inversion

In both experiments with either non-selective or slab selective inversion, all static tissues within the imaging volume are inverted and show identical signal behavior over time. Inflowing blood, however, is only exposed to the non-selective inversion. By subtraction of the two datasets, static signal from background tissues is cancelled out, but inflowing blood appears with bright signal due to the difference between inverted and non-inverted blood. The time series of subtracted 3D datasets were then subjected to inline MIP processing in the axial, sagittal and coronal plane.

4D SSFP MRA consisted of 48 tilted axial slices that covered the carotid siphon and the basilar artery as well as the anterior, middle and posterior cerebral artery. 15 temporal phases with a temporal resolution of 115 ms were acquired in 22 of 23 MR examinations. In the first MR examination of the patient that was examined twice, 10 temporal phases with a temporal resolution of 115 ms were acquired. The other imaging parameters were as follows: field of view (FOV) 165×220 mm², voxel size $1.2 \times 1.0 \times 1.0$ mm³, TR 115 ms, TE 1.4 ms, flip angle 39°, bandwidth 745 Hz/pixel, parallel imaging GRAPPA=2. Acquisition time for 4D SSFP MRA ranged from 4-6 min, pending on the heart rate.

Image analysis

All MR images were analyzed by two radiologists blinded to the results of DSA in consensus mode.

Anterior collateral flow was diagnosed when there was crossover circulation from the internal carotid artery to the contralateral cerebral hemisphere via the anterior communicating artery. Posterior collateral flow was reported when there was retrograde filling of the anterior circulation via the right or left posterior communicating artery (PComA) or retrograde filling of the basilar artery via the right or left posterior communicating artery. In addition, the visualization of collateral supply via a patent EC-IC bypass was documented.

In addition, subjective image quality of axial MIP reconstructions of 4D SSFP MRA was assessed in patients without an EC-IC bypass (n=15) independently for the following predefined vessel segments: M1 segment of the middle cerebral artery (MCA) (from internal carotid artery

bifurcation to main division of the MCA); M2 segment of MCA (from main division to insula); M3 segment of MCA (from insula to opercular turn of MCA branches); A1 segment of anterior cerebral artery (from internal carotid artery bifurcation to anterior communicating artery); A2 segment of anterior cerebral artery (from anterior communicating artery to genu of corpus callosum); P1 segment of posterior cerebral artery (from basilar artery bifurcation to posterior communicating artery); P2 segment of posterior cerebral artery (from posterior communicating artery to back of midbrain); P3 segment of posterior cerebral artery (from back of midbrain to division into posterior temporal and parieto-occipital arteries). In addition, subjective image quality was assessed for the distal internal carotid artery (ICA).

For each segment, subjective image quality was rated independently by two radiologists using a four-point scale as follows: 4=excellent (sharp and complete delineation of vessel borders, homogenous vessel signal without artifacts), 3=good (good delineation of vessel borders with slight irregularities, homogenous vessel signal with slight artifacts), 2=fair (vessel borders scarcely definable, inhomogeneous vessel signal) and 1=non-diagnostic (vessel borders not definable).

Statistical analysis

The Statistical Package for Social Sciences (SPSS for Windows Package 15.0, Chicago, IL) was used for statistical analysis and calculation of mean values and standard deviations. DSA served as the reference standard for calculation of sensitivity, specificity as well as positive and negative predictive value of 4D SSFP MRA.

κ-values were used to determine agreement for subjective image quality between both readers. A value of less than 0.50 corresponds to poor agreement; a value of 0.50–0.75 corresponds to good agreement and a value greater than 0.75 corresponds to excellent agreement.

Results

One patient was excluded, as 4D SSFP MRA failed to visualize the cerebral arteries due to severe motion during
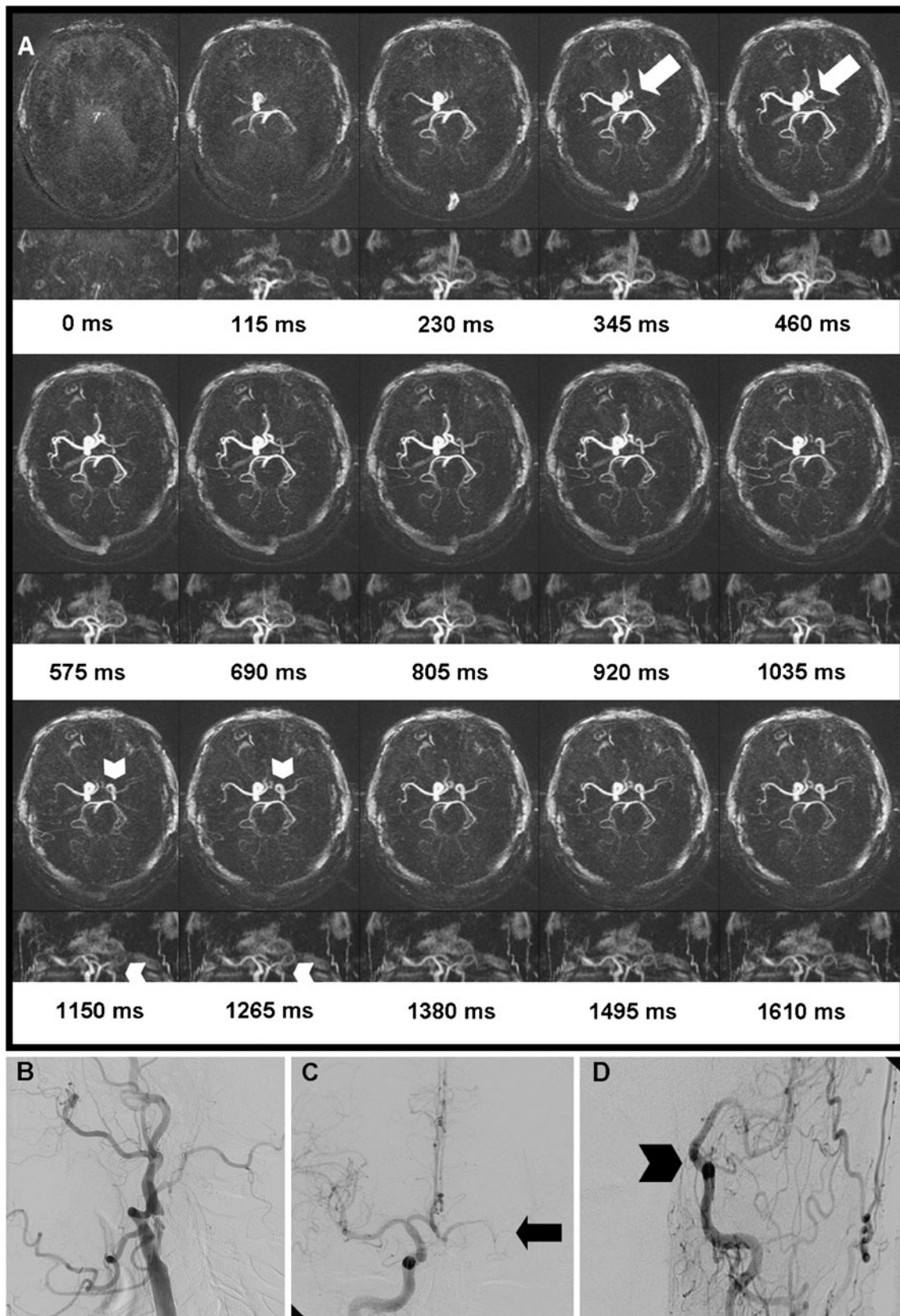
Fig. 2 72-year-old male patient with severe stenosis of the left ICA (**b**). 4D SSFP MRA shows anterior collateral flow (*arrow*) to the left MCA (**a**), which is confirmed by DSA (**c**). In addition, delayed residual antegrade flow is seen in the distal left ICA (arrowhead) with both 4D SSFP MRA (**a**) and DSA (**d**)

the acquisition. Image acquisition was completed successfully in 21 of 22 patients (95.5%), which were considered for further analysis.

In 17 patients, DSA detected anterior collateral flow ($n=$8) (Fig. 2), posterior collateral via the right ($n=8$) and left ($n=7$) posterior communicating artery as well as patent EC-IC bypasses ($n=8$)(Table 1). In addition, DSA disclosed retrograde filling of the basilar artery in 2 patients (Fig. 3) and delayed antegrade flow in the ICA without collateral supply in one patient. Consistently, with both DSA and 4D SSFP MRA no collateral pathways were found in 4 patients (Fig. 4), including one patient with a severe stenosis of the right ICA (Table 1). 29 of 31 collateral pathways were dynamically visualized with 4D SSFP MRA. In one patient with bilateral EC-IC bypass, only the left EC-IC bypass was identified with 4D SSFP MRA. In addition, in one patient with moyamoya disease and bilateral PcomA collateral flow from the posterior to the anterior circulation, collateral flow was only visible in the left PcomA with 4D SSFP MRA. In the patient that was examined twice, no collateral flow was visible

following stent placement in the right ICA. However, as the posterior circulation and the left ICA were not visualized by DSA following stenting, the second MR examination was not considered for analysis (Fig. 5).

Absence of anterior collateral flow ($n=13$) or posterior collateral flow via the left ($n=14$) or right ($n=13$) posterior communicating artery was correctly diagnosed with 4D SSFP MRA.

As compared to DSA, a sensitivity of 93.5% (95% confidence interval: 77%, 99%), specificity of 100% (95% confidence interval: 89%, 100%), positive predictive value (PPV) of 100% (95% confidence interval: 85%, 100%) and negative predictive value (NPV) of 95.2% (95% confidence interval: 83%, 99%) were calculated for dynamic visualization of collateral flow with 4D SSFP MRA.

Mean image quality for segments ICA, M1, A1, P1 and P2 was excellent (3.80 ± 0.40, 3.73 ± 0.40, 3.60 ± 0.52, 3.70 ± 0.44 and 3.53 ± 0.50, respectively). In contrast, image quality for segment A2 was only considered acceptable (2.43 ± 0.91). M3 branches were visible in 13 of 15 patients

Table 1 Clinical data and patterns of collateral flow as assessed with 4D SSFP MRA and DSA

| Patient No.	Age	Collateral flow 4D SSFP MRA	Collateral flow DSA	Underlying pathology as assessed by DSA
1	57	Anterior, PcomA (r)	Anterior, PcomA (r)	Severe stenosis of right ICA
2	71	PcomA (r)	PcomA (r)	Severe stenosis of right ICA
3	74			Severe stenosis of right ICA
4	73			Occlusion of left vertrebral artery
5	48	Anterior, EC/IC (l), retrograde flow in basilar artery	Anterior, EC/IC (l), retrograde flow in basilar artery	Occlusion of left ICA and of both vertebral arteries
6	59	Anterior, PcomA (l)	Anterior, PcomA (l)	Occlusion of left ICA
7	40	EC-IC (l)	EC-IC (l)	Moyamoya disease
8	71	PcomA (l), delayed antegrade flow in ICA and MCA (r)	PcomA (l), delayed antegrade flow in ICA and MCA (r)	Severe stenosis of proximal right ICA, moderate stenosis of left ICA, hypoplastic left P1 segment
9	61	Anterior	Anterior	Occlusion of right ICA, severe stenosis of left ICA
10	38	EC-IC (r,l), PcomA (l)	EC-IC (r,l), PcomA (r,l)	Moyamoya disease
11	51	EC-IC (l), PcomA (r,l)	EC-IC (l), PcomA (r,l)	Occlusion of left ICA, pseudoocclusion of right ICA
12	77			Following surgery of an aneurysm of the left vertebral artery
13	41	Anterior, EC-IC (l)	Anterior, EC-IC (l)	Occlusion of left ICA
14	48	PcomA (r), retrograde flow in basilar artery	PcomA (r), retrograde flow in basilar artery	Occlusion of basilar artery
15	52	EC-IC (l), PcomA (r,l)	EC-IC (r,l), PcomA (r,l)	Moyamoya disease
16	71			Mild stenosis of left ICA
17	52	PcomA (l)	PcomA (l)	Occlusion of left ICA
18	52	PcomA (r)	PcomA (r)	Severe stenosis of right ICA
19	72	Anterior	Anterior	Severe stenosis of left ICA
20	67	Anterior, PcomA (l)	Anterior, PcomA (l)	Occlusion of left ICA
21	56	Anterior, PcomA (r)	Anterior, PcomA (r)	Occlusion of right ICA

Anterior - collateral flow via the anterior circulation

PcomA - collateral flow via the right (r) of left (l) posterior communicating artery

EC-IC - collateral flow via a right-sided (r) or left-sided (l) extracranial-intracranial bypass

Fig. 3 48-year-old patient with an occlusion of the left internal carotid artery and distal occlusion of both vertebral arteries as well as an extracranial-intracranial bypass on the left side (*arrow*). 4D SSFP MRA (**a**) discloses anterior collateral flow from the right internal carotid artery to the left middle cerebral artery. (**b**) In addition, collateral flow via the right PcomA to the posterior circulation with retrograde filling of the basilar artery (*arrowhead*) is seen with 4D SSFP MRA (**a**) and confirmed by DSA (**c**). Collateral flow via the patent EC/IC bypass (*arrow*) is visualized with both 4D SSFP MRA (**a**) and DSA (**d**)
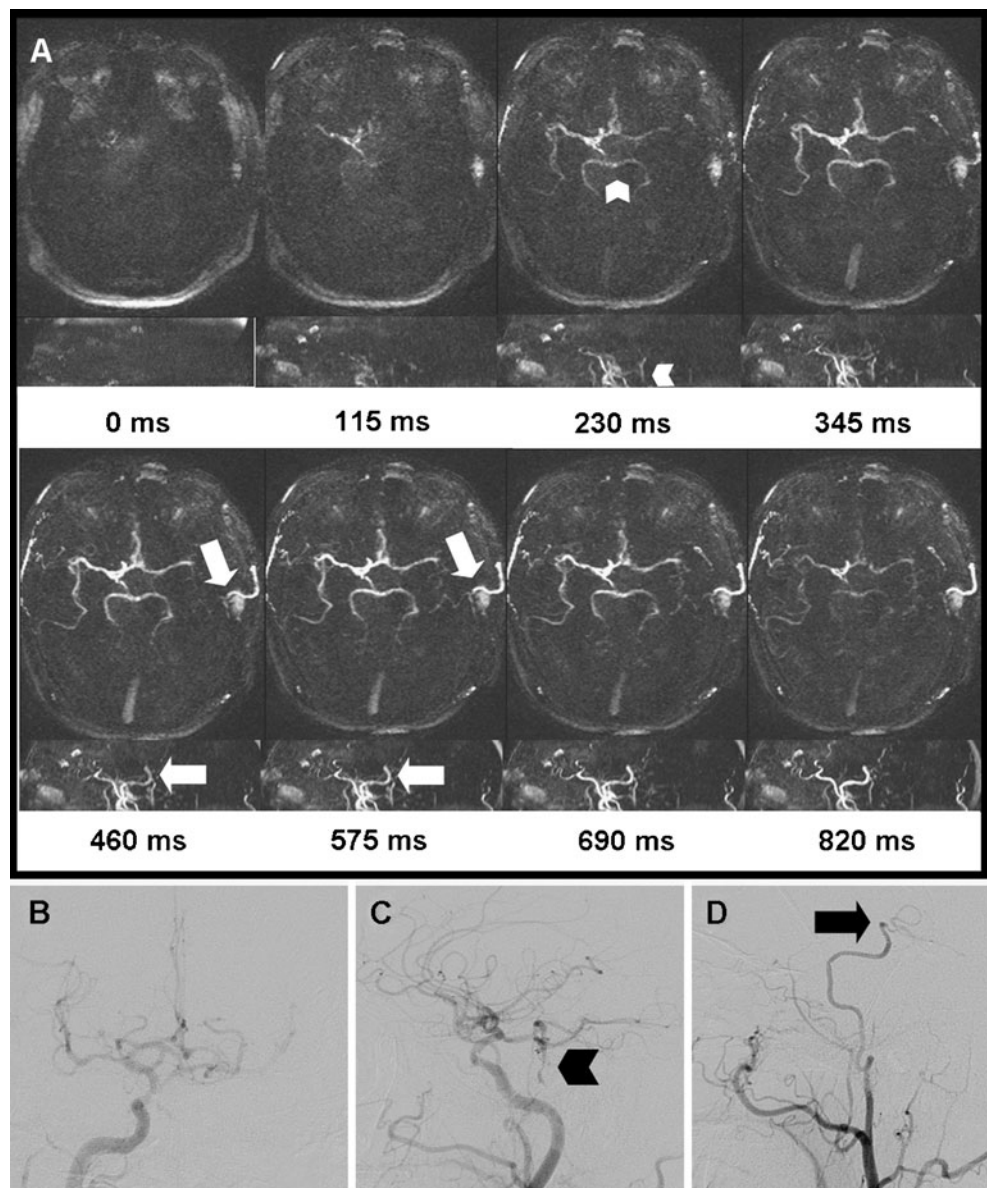
(86.7%) and P3 branches were visible in 14 of 15 patients (93.3%) considered for subjective image quality analysis. Mean image quality for segments M3 and P3 was 2.30 ± 0.73 and 2.60 ± 0.58, respectively (Table 2). Kappa value for overall interobserver agreement was 0.85.

Discussion

In this study we have successfully applied a nonenhanced 4D SSFP MRA for dynamic visualization of intracranial collateral flow in patients with steno-occlusive disease of brain-supplying arteries.

Assessment of cerebral collateral flow is important in patients with steno-occlusive disease, as it might have prognostic implications [3]. The presence of collateral circulation might reduce the risk of hemispheric stroke or transient ischemic attack (TIA) in patients with severe ICA stenosis [19], as the collateral flow might improve cerebral perfusion and protect the brain from small thromboemboli [20, 21]. In addition, in patients with an acute ischemic stroke, the presence of intracranial collateral flow is associated with a reduced infarct volume and a better clinical outcome [22–24].

4D SSFP MRA has shown a high sensitivity and specificity for detection of primary collateral flow in patients with steno-occlusive disease in this study and might therefore contribute to non-invasive assessment of intracranial flow characteristics in patients with steno-occlusive disease.

As compared to time-resolved 4D contrast-enhanced MR angiography (4D CE-MRA), 4D SSFP has several advan-

Fig. 4 71-year-old male patient referred to DSA for sonographically suspected severe stenosis of the left ICA. Simultaneous filling of the right and left MCA is seen with 4D SSFP MRA (**a**). The anterior cerebral arteries are both supplied by the left ICA (**d**, *arrow*) and are timely visualized by 4D SSFP MRA (**a**, *arrow*). No collateral flow to the left hemisphere is found with both 4D SSFP MRA and DSA (**a**,**c**). No severe stenosis of the left ICA is seen on DSA (**b**)
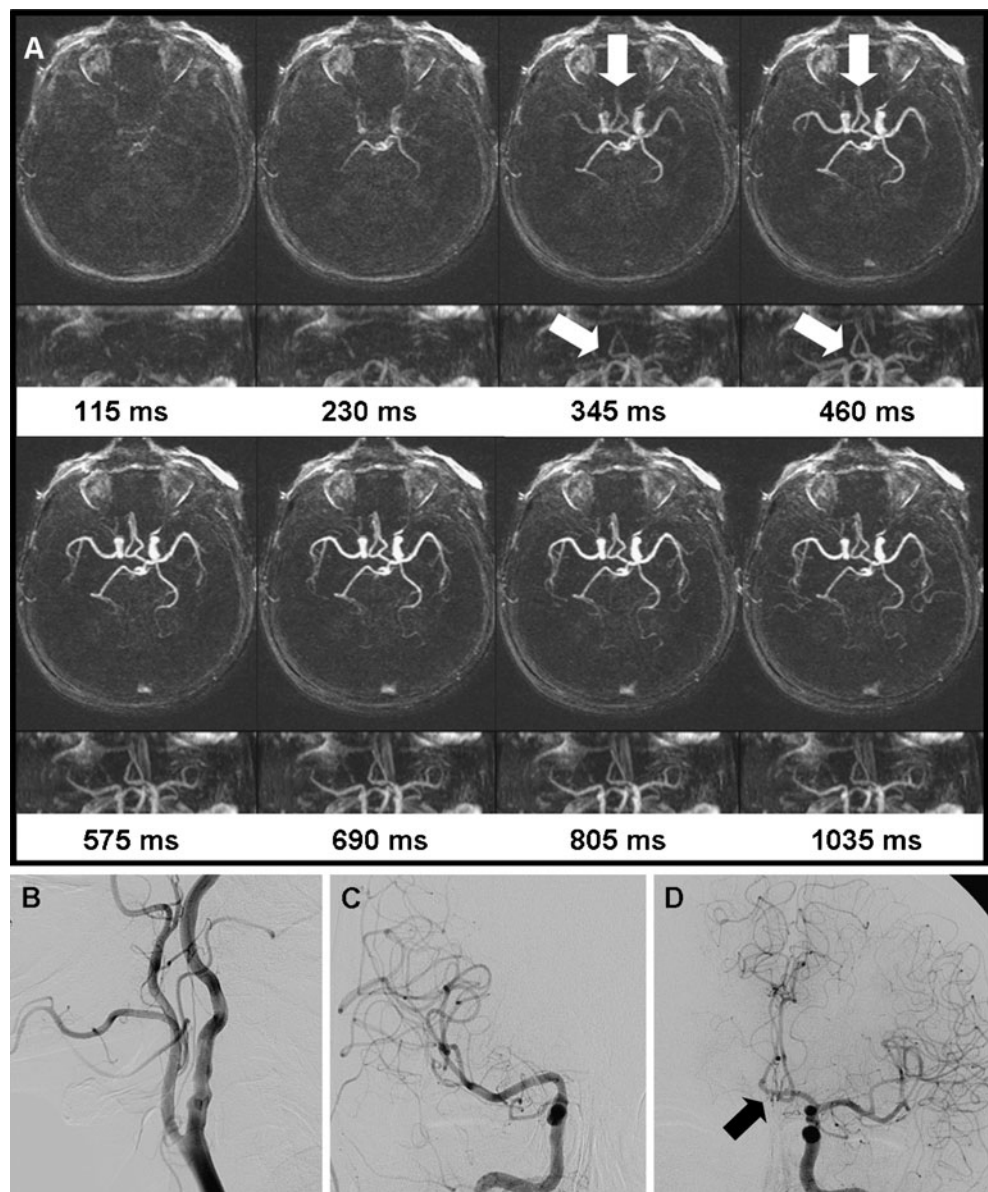

tages. The temporal resolution applied in this study (115 ms) is higher than the temporal resolution generally obtained with 4D CE-MRA [5–7]. Furthermore, 4D SSFP MRA is totally non-invasive, as it does not require the administration of gadolinium-based contrast material. Therefore, image acquisition is no longer confined to the contrast material bolus. Different regions can be studied with very high temporal resolutions and image acquisitions can be repeated in case of poor image quality.

In addition, there is a causal relationship between the administration of gadolinium-based contrast material and the development of nephrogenic systemic fibrosis in patients with a GFR of less than 30 ml/min/1.73m^2 [7, 8]. The prevalence of chronic kidney disease is significantly higher in patients at risk for stroke than among the general population [25]. As a nonenhanced imaging technique, 4D SSFP MRA can be performed safely in patients with contraindications for contrast material.

Recently, alternative nonenhanced imaging strategies have been introduced to assess intracranial collateral circulation, e.g. time-resolved 3D phase-contrast MR imaging (PC-MRI) and territorial arterial spin labeling MR imaging.

With time-resolved 3D PC-MRI, both flow velocities and the direction of blood in cerebral arteries can be assessed simultaneously [26, 27]. However, prolonged MR data acquisition times of 10-20 min and mainly time consuming post-processing have so far limited its use in the clinical routine. Territorial arterial spin labelling (ASL) allows for selective labelling of major brain-supplying arteries and therefore assessment of their perfusion territories [28–30]. Initial results on territorial ASL in patients
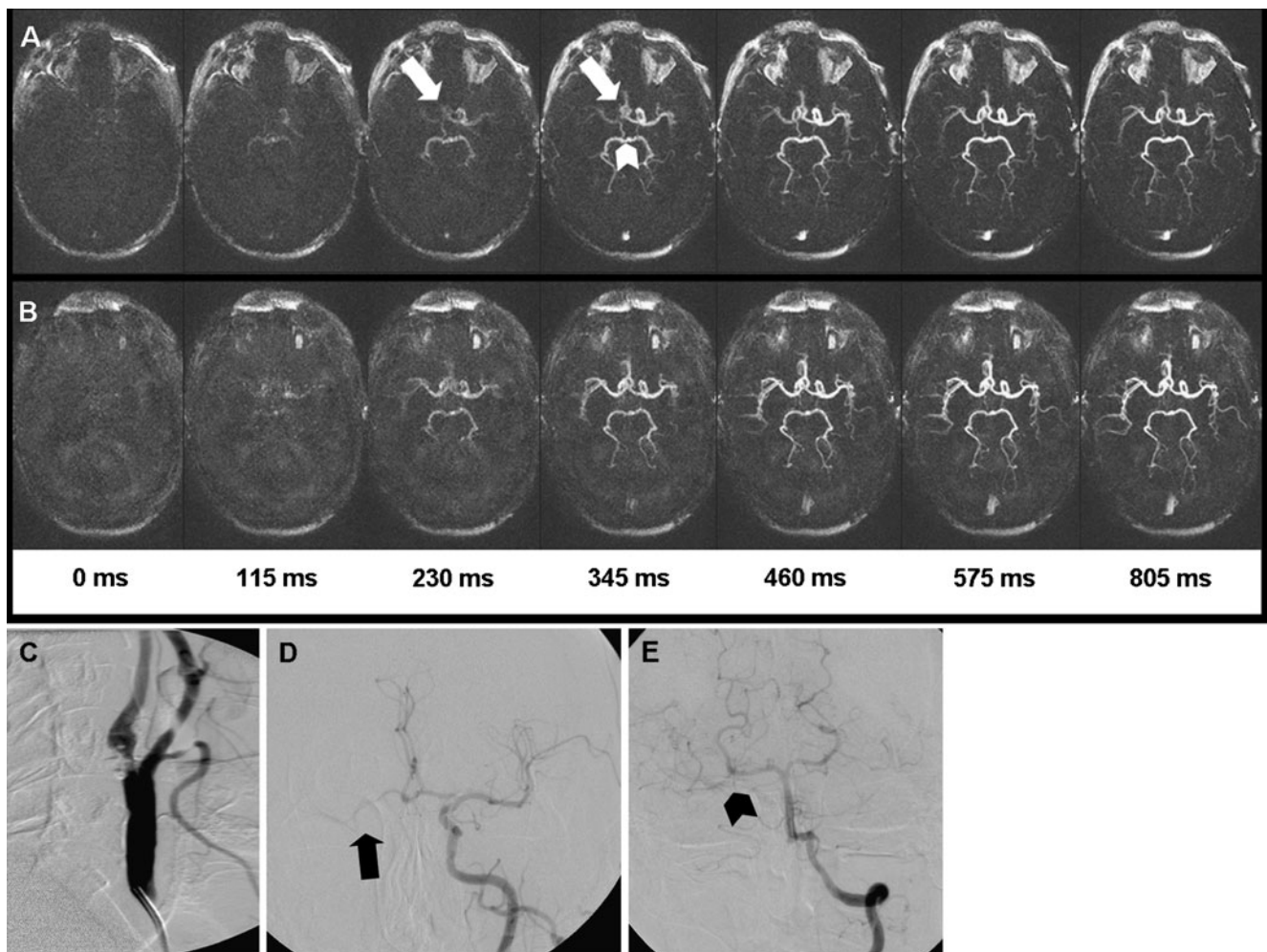
Fig. 5 57-year-old male patient with severe stenosis of the right ICA (c). Anterior collateral flow (*arrowhead*) and collateral flow via the right PcomA (*arrow*) with delayed visualization of the right MCA is seen with 4D SSFP MRA (a) and confirmed by DSA (d,e). Following stenting of the ICA stenosis, 4D SSFP MRA discloses simultaneous visualization of both MCA without collateral flow (b)

with steno-occlusive disease are very promising [28–30]. However, the need for selective labelling of several vessels lead to longer MR data acquisition times and complicate the post processing and interpretation of perfusion maps [29].

Table 2 Subjective image quality for predefined vessel segments on a 4-point scale (4=excellent; 1=not diagnostic)

Segment	Reader 1+2 (mean)	Reader 1	Reader 2
Distal ICA	3.80±0.40	3.80±0.41	3.80±0.41
M1	3.73±0.40	3.67±0.49	3.80±0.41
M2	3.40±0.69	3.33±0.72	3.47±0.74
M3	2.30±0.73	2.27±0.70	2.33±0.82
A1	3.60±0.52	3.67±0.49	3.53±0.64
A2	2.43±0.91	2.47±0.92	2.40±1.06
P1	3.70±0.44	3.73±0.46	3.67±0.49
P2	3.53±0.50	3.53±0.52	3.53±0.52
P3	2.60±0.58	2.60±0.63	2.60±0.63

Furthermore, territorial ASL does not provide direct information on vessel anatomy. By comparison, 4D SSFP MRA might provide both anatomical and hemodynamic information using a reasonably short MR sequence lasting 4–6 min. As axial, sagittal and coronal MIP images are immediately available for analysis due to in-line post processing [17] this imaging technique can be easily implemented in routine clinical care.

In previous studies, dynamic MR angiographies were obtained using pulsed arterial spin labelling in combination with a turbo fast low-angle shot (FLASH) or an echo-planar imaging (EPI) based Look-Locker sequence [31–33]. However, in these studies axial 2D sequences were applied, which did not allow for coronal and sagittal reconstructions. Furthermore, with a SSFP approach higher SNR and CNR can be obtained and image distortions and flow-related artifacts can be reduced as compared to the Look-Locker approaches [17].

The imaging technique presented in our study suffers from several limitations. With 4D SSFP MRA the depicted

vessel length depends on flow velocity and the delay time after spin labelling. Therefore, it seems not to be suitable for large coverage in the direction of blood flow, as for example the cervical arteries.

Furthermore, with the FAIR arterial spin labelling technique venous inflow from the upper border of the acquisition window is visualized. Although the venous inflow did not influence the visualization of the cerebral arteries on axial and sagittal MIP reconstructions, it hampered the evaluation of the cerebral arteries on coronal MIP reconstructions. Further developments in post processing should enable to perform selective MIP reconstructions for predefined vessels and to exclude venous structures in the MIP projections in the future. Alternatively, the use of different arterial spin labelling schemes, as for example signal targeting with alternating radiofrequency (STAR) ASL [34], might also avoid venous inflow.

Our study suffers from several further limitations. We acquired 15 temporal phases with a temporal resolution of 115 ms, enabling to cover a time frame of approx. 1700 ms with 4D SSFP MRA. However, with 4D SSFP MRA a higher temporal resolution in the order of 50 ms is achievable [16]. A higher temporal resolution might theoretically improve the visualization of collateral flow, but within a reasonable acquisition time, it is associated with a shorter time frame. In order not to miss delayed flow in cerebral arteries (Fig. 2), we performed 4D SSFP MRA with a temporal resolution of 115 ms in this study.

In addition, the inferior border of our tilted axial acquisition slab covered the basilar artery and the carotid siphon, but did not include the distal portion of the vertebral arteries and the entire orbit. Therefore, we were not able to evaluate secondary collateral flow patterns, as for example via the ophthalmic artery [3]. Furthermore, we did not evaluate the presence of leptomeningeal collaterals in this study, as the imaging slab did not cover the entire brain and the image quality of peripheral vessel segments was not diagnostic in all patients. The use of variable flip angles at 3 T has shown a substantial improvement in the visibility of peripheral vessel segments with 4D SSFP MRA in healthy subjects and future studies should address this issue [35].

In conclusion, with time-resolved 4D SSFP MRA, both the anatomical structure and dynamic filling of cerebral arteries can be assessed reliably. Therefore, it can provide relevant hemodynamic information in patients with steno-occlusive disease of brain supplying arteries. As a non-enhanced imaging technique it can be applied safely in patients with contraindication for contrast agents.

References

1. Rosamond W, Flegal K, Furie K et al (2007) Heart disease and stroke statistics: 2007 update—a report from the American Heart Association statistics committee and stroke statistics subcommittee. Circulation 115:e172
2. Halliday A, Mansfield A, Marro J, Peto C, Peto R, Potter J, Thomas D, MRC Asymptomatic Carotid Surgery Trial (ASCT) Collaborative Group (2004) Prevention of disabling and fatal strokes by successful carotid endarterectomy in patients without recent neurological symptoms: randomised controlled trial. Lancet 363:1491–502
3. Liebeskind DS (2003) Collateral circulation 34:2279–84
4. Kaufmann TJ, Huston J III, Mandrekar JN, Schleck CD, Thielen KR, Kallmes DF (2007) Complications of diagnostic cerebral angiography: evaluation of 19, 826 consecutive patients. Radiology 243:812–819
5. Hadizadeh DR, von Falkenhausen M, Gieseke J, Meyer B, Urbach H, Hoogeveen R, Schild HH, Willinek WA (2008) Cerebral arteriovenous malformation: Spetzler-Martin classification at subsecond-temporal-resolution four-dimensional MR angiography compared with that at DSA. Radiology 246:205–13
6. Willinek WA, Hadizadeh DR, von Falkenhausen M, Urbach H, Hoogeveen R, Schild HH, Gieseke J (2008) 4D time-resolved MR angiography with keyhole (4D-TRAK): more than 60 times accelerated MRA using a combination of CENTRA, keyhole, and SENSE at 3.0 T. J Magn Reson Imaging 27:1455–60
7. Lim RP, Shapiro M, Wang EY, Law M, Babb JS, Rueff LE, Jacob JS, Kim S, Carson RH, Mulholland TP, Laub G, Hecht EM (2008) 3D time-resolved MR angiography (MRA) of the carotid artery with time-resolved imaging with stochastic trajectories: comparison with 3D contrast-enhanced bolus-chase MRA and 3D time-of-flight MRA. Am J Neuroradiol 29:1847–54
8. Grobner T (2006) Gadolinium—a specific trigger for the development of nephrogenic systemic fibrosing dermopathy and nephrogenic systemic fibrosis? Nephrol Dial Transplant 21:1104–8
9. Marckmann P, Skov L, Rossen K, Dupont A, Damholt MB, Heaf JG, Thomsen HS (2006) Nephrogenic systemic fibrosis: suspected causative role of gadodiamide used for contrast-enhanced magnetic resonance imaging. J Am Soc Nephrol 17:2359–62
10. Koktzoglou I, Edelman RR (2008) Fast projective carotid MR angiography using arterial spin-labeled balanced SSFP. J Magn Reson Imaging 28:778–829
11. Lanzman RS, Voiculescu A, Walther C, Ringelstein A, Bi X, Schmitt P, Freitag SM, Won S, Scherer A, Blondin D (2009) ECG-gated nonenhanced 3D steady-state free precession (SSFP) MR angiography (MRA) in assessment of transplant renal arteries: comparison with digital substraction angiography (DSA). Radiology 252:914–21
12. Katoh M, Spüntrup E, Kuehl H, Stuber M, Günther RW, Botnar RM (2009) Flow-targeted inversion-prepared b-TFE coronary MR angiography: initial results in patients. Fortschr Roentgenstr 181:1050–5
13. Glockner JF, Takahashi N, Kawashima A, Woodrum DA, Stanley DW, Takei N, Miyoshi M, Sun W (2010) Non-contrast renal artery MRA using an inflow inversion recovery steady-state free precession technique (Inhance): Comparison with 3D contrast-enhanced MRA. J Magn Reson Imaging 31:1411–1418
14. Maki JH, Wilson GJ, Eubank WB, Glickerman DJ, Pipavath S, Hoogeveen RM (2007) Steady-state free precession MRA of the renal arteries: breath-hold and navigator-gated techniques vs. CE-MRA. J Magn Reson Imaging 26:966–973
15. Edelman RR, Siewert B, Darby DG, Thangaraj V, Nobre AC, Mesulam MM, Warach S (1994) Qualitative mapping of cerebral

blood flow and functional localization with echo-planar MR imaging and signal targeting with alternating radio frequency. Radiology 192:513–20

16. Bi X, Weale P, Schmitt P, Zuehlsdorff S, Jerecic R (2010) Non-contrast-enhanced four-dimensional (4D) intracranial MR angiography: A feasibility study. Magn Reson Med 63:835–41

17. Yan L, Wang S, Zhuo Y, Wolf RL, Stiefel MF, An J, Ye Y, Zhang Q, Melhem ER, Wang DJ (2010) Unenhanced Dynamic MR Angiography: High Spatial and Temporal Resolution by Using True FISP-based Spin Tagging with Alternating Radiofrequency. Radiology 256:270–9

18. Kim SG (1995) Quantification of relative cerebral blood flow change by flow-sensitive alternating inversion recovery (FAIR) technique: application to functional mapping. Magn Reson Med 34:293–301

19. Henderson RD, Eliasziw M, Fox AJ, Rothwell PM, Barnett HJ, for the North American Symptomatic Carotid Endarterectomy Trial (NASCET) Group (2002) Angiographically defined collateral circulation and risk of stroke in patients with severe carotid artery stenosis. Stroke 31:128–132

20. Lopez-Bresnahan MV, Kearse LA, Yanez P, Young TI (1993) Anterior communicating artery collateral flow protection against ischemic change during carotid endarterectomy. J Neurosurg 79:379–382

21. Schneider PA, Ringelstein EB, Rossman ME, Dilley RB, Sobel DF, Otis SM, Bernstein EF (1988) Importance of cerebral collateral pathways during carotid endarterectomy. Stroke 19:1328–1334

22. Harrison MJ, Koch C, Eckert B, Becker V, Kromer H, Heesen C, Gryska U, Freitag HJ, Rother J, Zeumer H (2003) Collateral circulation is an independent radiological predictor of outcome after thrombolysis in acute ischemic stroke. Neuroradiology 45:11–18

23. Hendrikse J, Hartkamp MJ, Hillen B, Mali WPTM, van der Grond J (2001) Collateral ability of the circle of Willis in patients with unilateral internal carotid artery occlusion—Border zone infarcts and clinical symptoms. Stroke 32:2768–2773

24. Bisschops RHC, Klijn CJM, Kapelle LJ, van Huffelen AC, van der Grond J (2003) Collateral flow and ischemic brain lesions in patients with unilateral carotid artery occlusion. Neurology 60:1435–1441

25. Fried LF, Shlipak MG, Crump C, Bleyer AJ, Gottdiener SJ, Kronmal RA, Kuller LH, Newman AB (2003) Renal insufficiency

as a predictor of cardiovascular outcomes and mortality in elderly individuals. J Am Coll Cardiol 41:1364–72

26. Hope MD, Purcell DD, Hope TA, von Morze C, Vigneron DB, Alley MT, Dillon WP (2009) Complete intracranial arterial and venous blood flow evaluation with 4D flow MR imaging. Am J Neuroradiol 30:362–366

27. Wetzel S, Meckel S, Frydrychowicz A, Bonati L, Radue EW, Scheffler K, Henning J, Markl M (2007) In vivo assessment and visualization of intracranial arterial hemodynamics with flow-sensitized 4D MR imaging at 3 T. Am J Neuroradiol 28:433–438

28. Bokkers RPH, van Laar PJ, van de Ven KCC, Kapelle LJ, Klijn CJM, Hendrikse J (2008) Arterial spin-labeling MR imaging measurements of timing parameters in patients with a carotid artery occlusion. Am J Neuroradiol 29:1698–1703

29. Chng SM, Petersen ET, Zimine I, Sitoh YY, Lim CCT, Golay X (2008) Territorial arterial spin labeling in the assessment of collateral circulation: comparison with digital subtraction angiography. Stroke 39:3248–3254

30. Wu B, Wang X, Guo J, Xie S, Wong EC, Zhang J, Jiang X, Fang J (2008) Collateral circulation imaging: MR perfusion territory arterial spin labeling at 3 T. Am J Neuroradiol 29:1855–1860

31. van Osch MJ, Hendrikse J, Golay X, Bakker CJ, van der Grond J (2006) Non-invasive visualization of collateral blood flow patterns of the circle of Willis by dynamic MR angiography. Med Image Anal 10:59–70

32. Salustio F, Kern R, Günther M, Szabo K, Griebe M, Meairs S, Hennerici M, Gass A (2008) Assessment of intracranial collateral flow by using dynamic arterial spin labeling MRA and transcranial color-coded duplex ultrasound. Stroke 39:1894–1897

33. Warmuth C, Rüping M, Förschler A, Koennecke H, Valdueza JM, Kauert A, Schreiber SJ, Siekmann R, Zimmer C (2005) Dynamic spin labeling angiography in extracranial carotid artery stenosis. Am J Neuroradiol 26:1035–1043

34. Edelman RR, Siewert B, Adamis M, Gaa J, Laub G, Wielopolski P (1994) Signal targeting with alternating radiofrequency (STAR) sequences: application to MR angiography. Magn Res Med 31:233–8

35. Schmitt P, Speier P, Bi X, Weale P, Müller E (2010) Non-contrast-enhanced 4D intracranial MR angiography: Optimizations using a variable flip angle approach. Proceedings of the 18th ISMRM Scientific Meeting; Stockholm, Sweden: 402